

Pion scattering to 6^- stretched states in ^{32}S

B. L. Clausen and T. W. Johnson

*Geoscience Research Institute, Loma Linda University, Loma Linda, California 92350
and Department of Physics, La Sierra University, Riverside, California 92515*

R. A. Lindgren and K. Cromer

Institute of Nuclear and Particle Physics and Department of Physics, University of Virginia, Charlottesville, Virginia 22901

R. J. Peterson

Nuclear Physics Laboratory, University of Colorado, Boulder, Colorado 80309

A. D. Bacher

Indiana University Cyclotron Facility, Bloomington, Indiana 47408

H. Ward and A. L. Williams*

Department of Physics, University of Texas, Austin, Texas 78712

(Received 23 August 1996)

Inelastic π^\pm differential cross-section measurements at a pion incident energy of 162 MeV were made for 12 ($f_{7/2}d_{5/2}^- - 1$) 6^- states in ^{32}S , including four tentative new isoscalar states. Isoscalar and isovector magnetic structure coefficients were determined for each state by combining the pion data with previous electron scattering data. The trend of small isoscalar/isovector strength ratios continues in ^{32}S , with the isovector strength being comparable to theoretical calculations, but the isoscalar strength exhausting only about 17% of an extreme-single-particle-hole model. However, this isoscalar strength is larger than that observed in other sd -shell nuclei and exhausts 75% of large-basis shell-model predictions. The substantial fragmentation of the 6^- isovector strength observed in ^{32}S electron scattering, but not previously observed in other self-conjugate nuclei, appears to extend to the isoscalar strength and to include substantial isospin mixing. The general systematics of isoscalar and isovector stretched state transition strengths are reviewed.

[S0556-2813(97)00402-0]

PACS number(s): 25.80.Ek, 21.60.Cs, 27.30.+t

I. INTRODUCTION

High-spin stretched transitions, i.e., transitions with the highest angular momentum attainable in a single-particle transition between adjacent major shells, have been of interest because of the simplifying assumption that the one-body transition density is given by a simple unique particle-hole configuration. This makes it possible to compare nuclear structure models to experiment via one spectroscopic amplitude. This amplitude is deduced from (e, e') experiments in an almost model-independent way and also serves as a benchmark for comparison with results from other probes, such as (π, π') , (p, p') , and (p, n) . Several reviews [1,2] have summarized the importance of these studies.

Electron-scattering measurements [3] on ^{32}S identified several 6^- states of the type ($f_{7/2}d_{5/2}^- - 1$) and (p, n) charge exchange measurements [4] identified several 6^- isovector states, but the extracted strengths for the two lowest states in (p, n) were only about half as strong as those observed in (e, e') . Comparisons between the weaker higher lying states were consistent given the large errors on the measurements.

This is inconsistent with other nuclei like ^{28}Si , where the lowest states in both reactions are in approximate agreement. The ^{32}S nucleus is also different than other self-conjugate nuclei in that the observed strength is spread out over more states instead of being concentrated in one or two levels as in ^{28}Si [4-7], ^{24}Mg [4,8-10], and ^{20}Ne [4]. Additional (p, n) reactions on ^{40}Ca and ^{36}Ar have been used to study the fragmentation of these high-spin stretched states [11]. Clearly, we should understand the differences between the strengths extracted from the (e, e') and (p, n) reactions on ^{32}S .

In search of an explanation in terms of isospin mixing effects, we report on measurements of π^\pm scattering on ^{32}S and the determination of the isoscalar and isovector structure coefficients for the 6^- states. Since in pion scattering near the $\Delta_{3,3}$ resonance the intrinsic isoscalar amplitude is about a factor of 2 larger than the isovector amplitude and in electron scattering the intrinsic spin isovector amplitude is about a factor of 5 larger than the isoscalar amplitude, a consistent analysis of both sets of data for the same transition can be used to determine the isoscalar and isovector strength for pure and mixed isospin spin excitations such as these high-spin states. This combined electron-pion analysis can be more reliable for determining isoscalar strength than other methods. This has been demonstrated in previous measurements for stretched transitions in ^{12}C [12,13], ^{14}C [14,15],

*Present address: Johns Hopkins Oncology Center, Division of Radiation Oncology, 600 N. Wolfe Street, Baltimore, MD 21287.

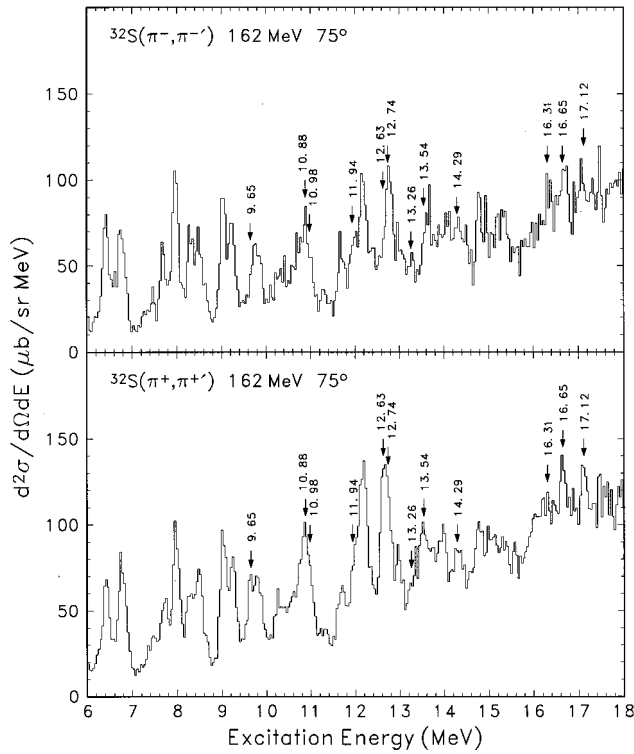


FIG. 1. Spectra from inelastic scattering of 162 MeV π^- and π^+ on ^{32}S at a laboratory scattering angle of 75° . The labeled states are 6^- stretched transitions. Each energy bin is 40 keV wide.

^{14}N [16,17], ^{16}O [18,19], ^{24}Mg [9,8], ^{26}Mg [20,21], ^{28}Si [22,23], ^{54}Fe [24,25], and ^{60}Ni [26,27].

The isoscalar and isovector structure coefficients extracted from the $^{32}\text{S}(\pi, \pi')$ data will be compared with results from large-basis shell-model (LBSM) calculations [28] and also with other nuclei, extending the systematics for $M6$ stretched transitions with the goal of improving our understanding of the quenching, fragmentation, and isospin mixing of the magnetic strength. Comparisons of pure isospin structure coefficients determined from a combination of pion and electron cross section measurements will aid in understanding the normalization of the pion-nucleon interaction in nuclei and the asymmetries in π^-/π^+ scattering to unbound states with asymmetric nucleon binding energies.

II. DATA ACQUISITION AND REDUCTION

This experiment was performed at the Clinton P. Anderson Meson Physics Facility (LAMPF) of the Los Alamos National Laboratory using 162-MeV π^+ and π^- . The target was enriched to 99.1% ^{32}S at the Oak Ridge National Laboratory with the remainder consisting of 0.2% ^{33}S and 0.7% ^{34}S . The target had an areal density of 100 mg/cm² and was enclosed between two aluminized Mylar sheets of areal density 0.9 mg/cm² each. Inelastic pion scattering data were taken at spectrometer angles of 55° , 75° , 90° , and 105° for π^+ and 75° and 90° for π^- using the Energetic Pion Channel and Spectrometer (EPICS) facility, described elsewhere [29]. These angles were expected to be near the maximum of the angular distribution for $M6$ excitations. Spectra with lower statistical accuracy were taken at 30° and 40° to en-

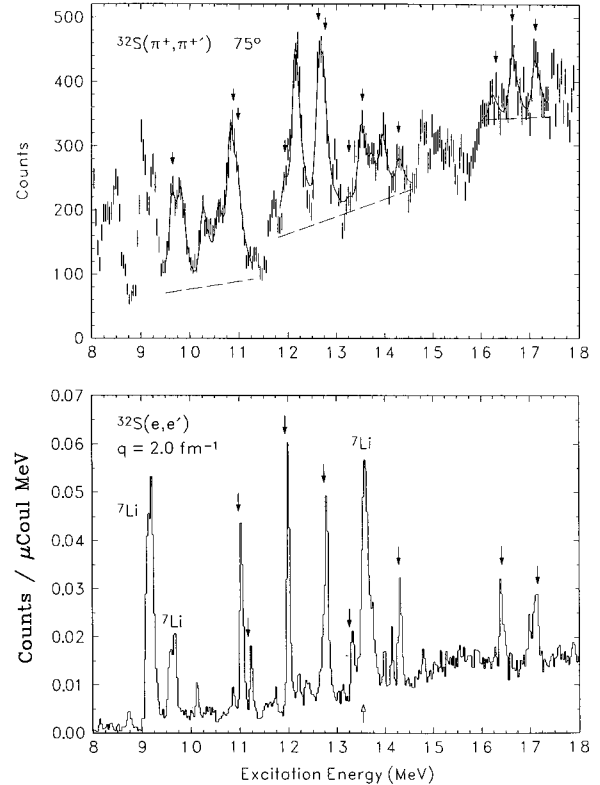


FIG. 2. Fits to the $^{32}\text{S}(\pi^+, \pi^+)$ spectrum at 75° , showing the backgrounds assumed. The spectrum has a resolution of about 170 keV. For comparison, the $^{32}\text{S}(e, e')$ spectrum at $q=2.0 \text{ fm}^{-1}$ is shown [3]. Its resolution is 100 keV. The 6^- stretched transitions are indicated by arrows.

sure that any angular distribution with a maximum at 75° was not a second maximum of a low multipolarity excitation. At most angles and for both π^+ and π^- , data were taken on targets of CH_2 and Mylar to determine the energy calibration and cross-section normalization. The resolution was enhanced by the use of, among other things, a thinner vacuum window and a reduced number of chamber planes in the front of the spectrometer [30]. The typical energy resolution was approximately 170 keV full width at half maximum (FWHM).

Representative spectra, corrected for spectrometer acceptance and pion survival, are shown in Fig. 1. Data analysis used the line-shape fitting program ALLFIT [31] with an empirical linear background connecting smooth regions of the spectra and a reference peak shape from an isolated low-lying state (see Fig. 2). The energy calibration at each angle utilized the prominent states in ^{12}C as well as known, low-lying ^{32}S states. The ^{32}S spectra included ^{12}C and ^{16}O peaks from the Mylar sheets enclosing the sulfur target. The location and size of these ^{12}C and ^{16}O excited states were determined from a plain mylar target and then fixed before fitting the ^{32}S peaks.

Excitation energies of the 6^- states in the pion scattering spectra are listed in Table I and compared with good concordance to those found previously with electron and proton scattering and the (p, n) reaction. All peaks are narrow relative to our resolution.

The 6^- cross sections were normalized to previously known $\pi+^{12}\text{C}$ and $\pi+^{16}\text{O}$ elastic-scattering cross sections

TABLE I. A comparison of excitation energies for ^{32}S 6^- stretched states from several different reactions. For the (π, π') states with no uncertainties listed, the peaks were either small or part of a doublet making an independent determination of the excitation energy impossible. A Coulomb shift of about 7.0025 MeV would be expected for the ^{32}Cl data based on the location of the analog of the ^{32}Cl ground state in ^{32}S [38].

E_x (MeV) (π, π')	E_x (MeV) (e, e') ^a	E_x (MeV) (p, p') ^b	E_x (MeV) $^{32}\text{S}(p, n)^{32}\text{Cl}$ ^c
9.65±0.03			
10.88±0.04			
10.98	10.98±0.04		3.8±0.1
	11.17±0.05		
11.94	11.94±0.04		4.7±0.1
12.63±0.03			
12.77±0.06	12.74±0.04		5.6±0.1
13.26	13.26±0.05	13.32	6.3±0.1
13.54±0.05	13.54±0.05		6.8±0.1
14.29	14.29±0.05		7.4±0.1
		15.75	8.4±0.1
16.31±0.07	16.43±0.07		9.2±0.1
16.65±0.07			
17.12±0.07	17.16±0.08		9.8±0.1

^aReference [3].

^bReference [37].

^cReference [4].

[32,33]. In an additional check, we found good agreement with previous ^{12}C inelastic-scattering cross sections [34] and with a $\theta_{\text{lab}} = 75^\circ$ $\pi^+ + p$ center-of-mass cross section of 8.48 mb/sr [35]. The normalization factor for the spectrometer

was smaller by a factor of 0.8 for π^- than for π^+ cross sections, similar to results found previously [29,26]. The total systematic error was about 8%, with 6% due to uncertainties in the absolute normalization. The pion-scattering cross

TABLE II. Center-of-mass π^+ scattering cross sections for states observed in ^{32}S . Scattering angles are given in the center-of-mass frame. The listed uncertainties include both statistical and systematic errors. An asterisk indicates where no peak was observed for an excited state at a particular scattering angle.

E_x (MeV)	J^π	σ^+ ($\mu\text{b/sr}$)					
		30.3°	40.4°	55.5°	75.6°	90.6°	105.6°
9.65 ^a	6^-	< 5	*	6.1±1.2	7.9±0.8	6.0±1.0	3.6±1.3
9.81		72.0±9.3	60.8±5.6	*	6.4±0.7	6.2±1.0	17.3±1.6
10.31		< 40	57.0±5.9	22.2±2.2	6.4±0.6	5.4±0.7	13.5±1.2
10.74		113±17	42.2±9.2	21.5±2.5	5.1±1.0	5.0±0.6	10.5±1.2
10.88 ^a	6^-	< 50	86.3±12	3.1±2.4	9.5±1.1	2.0±0.4	3.7±1.5
10.98	6^-	31.2±11	< 10	< 2	3.6±0.9	< 2	< 2
11.94	6^-	*	< 30	3.4±1.4	4.3±0.6	< 2	*
12.19		91.4±11	95.3±9.2	36.3±3.4	15.0±1.2	11.8±1.3	5.2±1.0
12.63 ^a	6^-	< 20	< 30	17.6±2.8	11.5±1.5	7.0±1.2	3.0±1.2
12.74	6^-	< 10	< 2	3.9±2.5	6.1±1.7	6.0±1.4	2.5±1.1
12.98		33.4±5.7	*	< 2	< 2	5.1±0.9	6.1±0.9
13.26	6^-	< 60	< 3	*	< 2	*	< 2
13.54	6^-	*	< 13	< 6	6.9±0.7	5.8±0.9	3.3±0.8
14.29	6^-	< 25	< 12	< 8	2.8±0.5	< 2	*
16.31	6^-	< 30	< 20	1.8±1.6	2.2±0.6	3.8±0.8	2.1±0.9
16.65 ^a	6^-	< 40	< 35	4.4±2.2	5.5±0.7	2.9±0.8	1.8±0.9
17.12	6^-	< 35	< 20	3.1±1.6	5.0±0.7	3.1±0.8	2.4±1.2

^aTentative new isoscalar state.

TABLE III. Center-of-mass π^- scattering cross sections for states observed in ^{32}S . Scattering angles are given in the center-of-mass frame. The listed uncertainties include both statistical and systematic errors. An asterisk indicates where no peak was observed for an excited state at a particular scattering angle.

E_x (MeV)	J^π	σ^- ($\mu\text{b}/\text{sr}$)	
		75.6°	90.6°
9.65 ^a	6^-	2.9 ± 1.3	3.1 ± 1.2
9.81		6.9 ± 1.5	7.5 ± 1.4
10.31		5.6 ± 0.8	5.8 ± 1.1
10.74		5.1 ± 0.6	5.0 ± 0.9
10.88 ^a	6^-	7.2 ± 0.7	< 2
10.98	6^-	2.1 ± 0.4	2.0 ± 0.8
11.94	6^-	3.9 ± 1.0	1.7 ± 1.2
12.19		9.1 ± 1.2	6.2 ± 1.3
12.63 ^a	6^-	2.8 ± 1.1	2.1 ± 1.4
12.74	6^-	10.2 ± 1.4	7.7 ± 1.9
12.98		1.9 ± 0.8	2.8 ± 1.5
13.26	6^-	< 2	*
13.54	6^-	1.9 ± 1.1	4.4 ± 1.3
14.29	6^-	3.1 ± 1.1	2.7 ± 1.2
16.31	6^-	2.9 ± 0.9	3.3 ± 1.6
16.65 ^a	6^-	4.8 ± 1.0	4.0 ± 1.4
17.12	6^-	4.1 ± 1.0	< 2

^aTentative new isoscalar state.

sections are listed in Tables II and III and plotted in Figs. 3 to 7 along with their errors that include both statistical and systematic uncertainties.

III. EXPERIMENTAL RESULTS

It is useful to have data from several different reactions for the self-conjugate ^{32}S nucleus in order to compare results

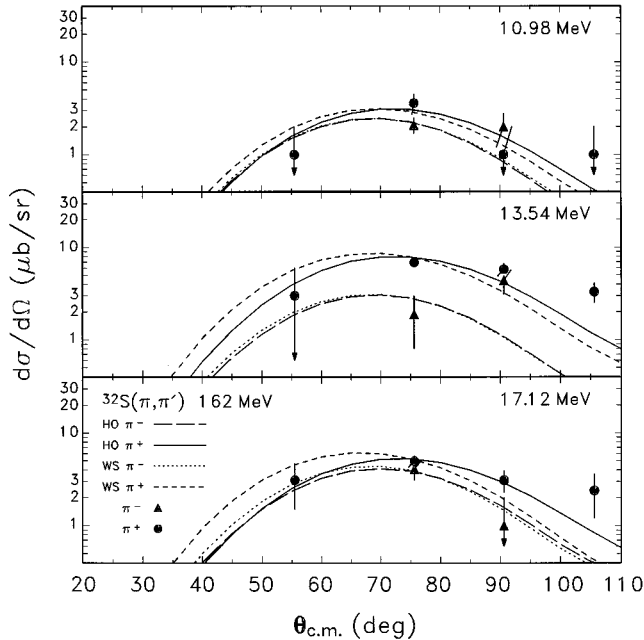


FIG. 3. Results from theoretical DWIA calculations using HO and WS wave functions are compared to each other and to π^\pm data for several ^{32}S 6^- isovector excitations.

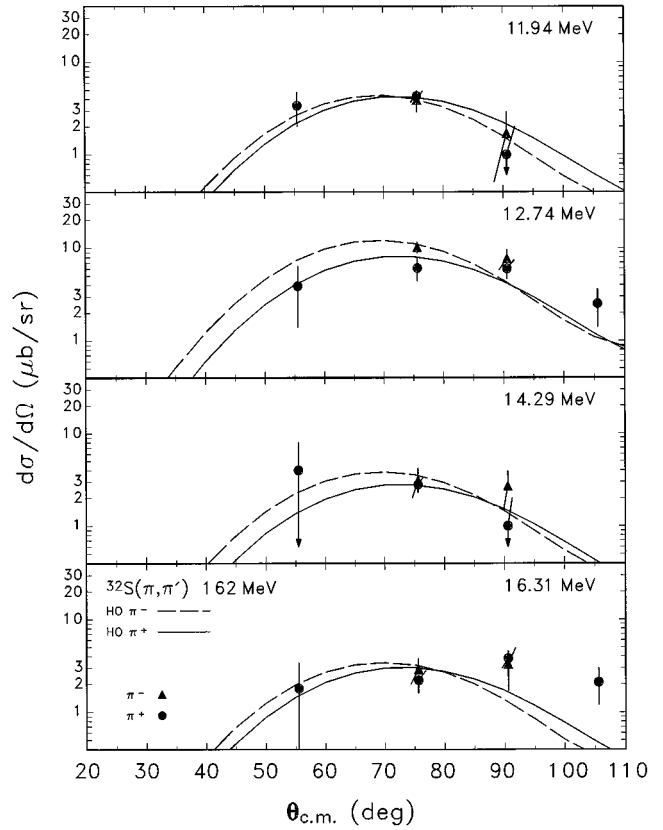


FIG. 4. The ^{32}S π^\pm data from several 6^- isovector excitations compared to theoretical DWIA calculations which used HO wave functions.

for the 6^- strength that is fragmented into several states. Each state will be discussed and the results from pion scattering and other reactions will be compared.

A. Isovector excitations

The 10.98 and 11.94 MeV transitions were strongly excited by electron scattering, and the corresponding 3.8 and 4.7 MeV states were two of the stronger ones observed with the (p,n) reaction; however, these two 6^- states were not prominent in the pion-scattering spectra. They were located on the shoulders of strong states at 10.8 and 12.2 MeV, so the fitting procedure had to fix the peak location for the expected 6^- state to obtain the cross sections plotted in Figs. 3 and 4. The resulting angular distributions are consistent with a 6^- assignment. The excitation energy of these two states approximately corresponds to the states at 11.29 and 11.84 MeV predicted from LBSM calculations [28,36].

The 11.17 and 13.26 MeV transitions were the two weakest states observed by electron scattering and were not observed at all in this pion-scattering experiment. No state was reported with the (p,n) reaction at 4.0 MeV which would correspond to the 11.17 MeV state. However, a prominent state was reported from the (p,n) reaction at 6.3 MeV that could correspond to the 13.26 MeV state, but possibly to the stronger 13.54 MeV state. A possible 6^- state was also reported at 13.32 MeV with (p,p') [37].

States of intermediate strength were observed at 13.54, 14.29, and 17.1 MeV with both electron and pion scattering,

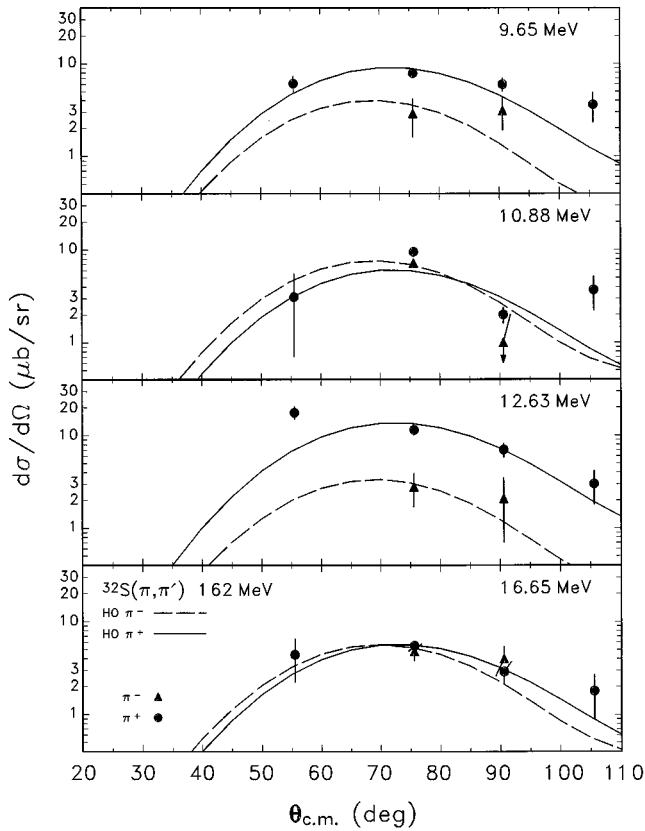


FIG. 5. The ^{32}S π^\pm data from possible new isoscalar 6^- excitations compared to theoretical DWIA calculations which used HO wave functions.

and the pion data are plotted in Figs. 3 and 4. Pion angular distributions are consistent with a 6^- assignment. The possible corresponding states from the (p, n) reaction at 6.8, 7.4, and 9.8 MeV are some of the weaker states in that reaction as well. The 13.54 MeV state corresponds to a LBSM prediction for a state at 13.42 MeV.

The weakest state reported from the (p, n) reaction, located at 8.4 MeV, has no corresponding state in either the electron or pion spectra near 15.4 MeV. However, preliminary data from a (p, p') reaction found a possible 6^- state at 15.75 MeV [37].

B. Isospin mixed excitations

The 12.74 MeV state is one of the strongest 6^- states observed by electron scattering, and the corresponding state at 5.6 MeV is the strongest from the (p, n) reaction. This experimentally located state corresponds to a LBSM state predicted at 12.74 MeV. This state was strongly excited by π^- , but less so by π^+ , as seen in Fig. 4. It appears to be isospin mixed with another strong state at 12.63 MeV which is strongly excited by π^+ , but much less so by π^- , as seen in Fig. 5. Figure 6 shows that the 12.63 MeV state is reasonably consistent with a 6^- angular distribution, although a 5^- assignment cannot be ruled out. The 12.74 MeV state in the electron-scattering spectra is unusually wide at the base [3], suggesting that the 12.63 MeV state is in fact weakly excited by electron scattering. Two-state isospin mixing in a self-conjugate nucleus has previously been observed for the

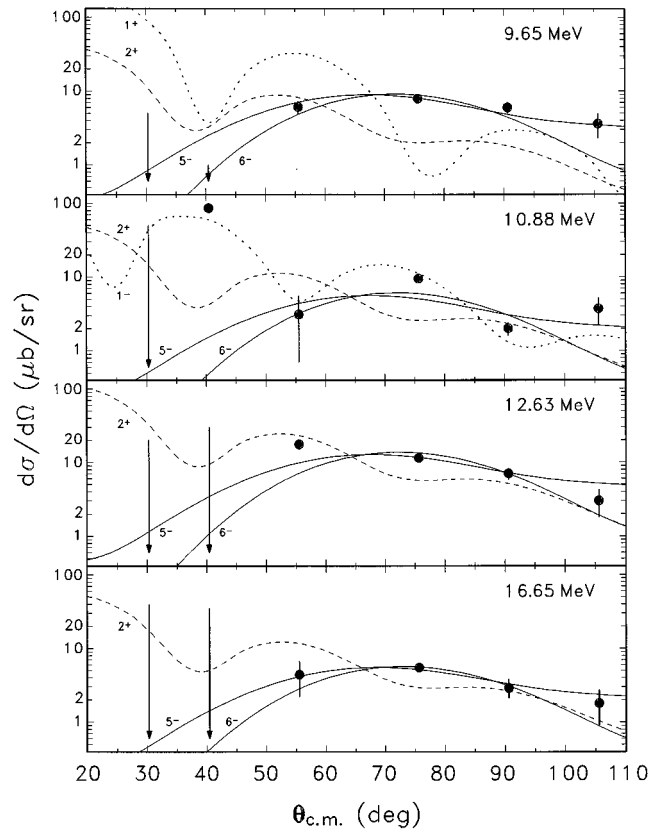


FIG. 6. Theoretical DWIA calculations using HO wave functions are shown for several multipolarities and compared with the ^{32}S π^+ data from the possible new isoscalar 6^- excitations.

19.5 MeV complex in ^{12}C , where similarly the lower state was protonlike and the upper state was neutronlike [12]. The mixing in ^{32}S is not as complete as that in ^{12}C , since both states are observed in both π^+ and π^- ^{32}S spectra. Using the definition in Ref. [12], the mixing coefficient $|\beta| = 0.2 \pm 0.1$.

A state was observed at 16.43 MeV in electron scattering and a corresponding state was observed at 9.2 MeV with the

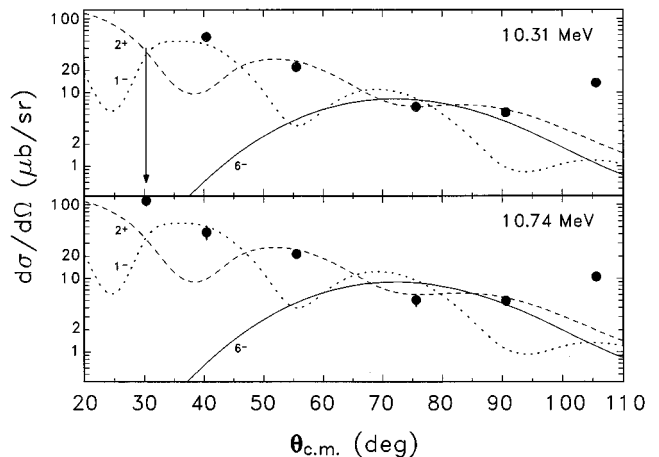


FIG. 7. Theoretical DWIA calculations using HO wave functions are shown for several multipolarities to compare with the ^{32}S π^+ data for sample lower multipolarity excitations.

(p,n) reaction. No state was observed at 16.43 MeV in the pion-scattering spectra; however, two other states were located at 16.31 and 16.65 MeV and their angular distributions are shown in Figs. 4 and 5, respectively. This is reminiscent of the three-state isospin mixing found near 16 MeV in ^{14}N [16,17] and near 19 MeV in ^{16}O [18,19]: one stretched state found by electron scattering with an additional state on either side found by pion scattering. However, all three states of the triplet in ^{14}N and ^{16}O were found with pion scattering, whereas only the lower and upper states were found in ^{32}S . Thus we treat the 16.31 ± 0.07 and 16.43 ± 0.07 MeV states as equivalent, considering that their excitation energies are equal within uncertainties. The 16.65 MeV state is then treated as a possible new 6^- isoscalar excitation. Its angular distribution displayed in Fig. 6 is reasonably consistent with such an assignment, although a 5^- assignment cannot be ruled out. This is probably another isospin mixed pair of states, with the lower excited slightly more strongly by π^- and the upper more strongly by π^+ . In the electron-scattering spectra, the 16.43 MeV peak was correspondingly found to be wider than some of other 6^- peaks.

C. Isoscalar excitations

Based on LBSM predictions of additional isoscalar strength around 10 MeV [28,36], seven additional states between 9 and 13 MeV were analyzed in a search for other possible 6^- transitions. Any new 6^- state, not observed by electron scattering, would be predominantly isoscalar. The (π, π') cross sections for these seven possible states are listed in Tables II and III. Five of the states, with excitation energies of 9.81 ± 0.03 , 10.31 ± 0.03 , 10.74 ± 0.04 , 12.19 ± 0.03 , and 12.98 ± 0.03 MeV, have experimental angular distributions at small angles incompatible with a 6^- assignment. As an example, data for the 10.31 and 10.74 MeV states are shown in Fig. 7 and compared to a 6^- calculation and several lower multipolarity calculations. The 10.31 MeV state may be a combination of a previously observed 2^+ excitation at 10.29 MeV and a 1^- excitation at 10.33 MeV. Similarly, the 10.74 MeV state may be a combination of a 1^- excitation at 10.70 MeV and a 2^+ excitation at 10.76 MeV [38].

A state at 9.65 MeV in the ^{32}S spectra is a possible 6^- excitation. It cannot be the 1^+ excitation observed at 9.66 MeV by electron scattering [39] and proton scattering [40] or the 2^+ state at 9.65 MeV found in several other reactions [38,41]. These lower multipolarity states would be strongly excited at small scattering angles, but no state was observed in our 30° and 40° spectra at this excitation energy. The data are compared to several theoretical calculations in Fig. 6, showing that a 6^- assignment for this state is reasonable, although a 5^- assignment might be possible. Corresponding LBSM theoretical predictions are for a 6^- isoscalar state at 9.21 MeV.

A ^{32}S state at 10.88 MeV is the remaining possibility for a 6^- assignment, and appears to be the only possibility of fitting the LBSM theoretical prediction of a strong isoscalar state at 10.36 MeV and a weaker state at 10.94 MeV. The data for the 10.88 MeV state shown in Fig. 6 have an angular distribution between 55° and 105° that would make a 6^- assignment reasonable. If this is a 6^- state, it has the most

isoscalar strength of any in ^{32}S . As would be expected, no state was reported at this excitation energy from electron scattering, nor at the corresponding energy for the (p,n) reaction, both of which selectively excite isovector transitions. However, the 6^- assignment for this state is somewhat questionable, since the 40° pion-scattering spectrum shows a strong state located at 10.90 ± 0.01 MeV. This may be an $L=1$ or $L=2$ state previously observed at 10.83 or 10.9 MeV [38,39,41], since the 1^- theoretical distribution shown in Fig. 6 fits the data reasonably well.

The states at 12.63 and 16.65 MeV discussed in the previous section and the 9.65 and 10.88 MeV states discussed in this section will be included in the calculations of total isoscalar 6^- strength, while recognizing that some of the 6^- assignments are tentative.

IV. ANALYSIS

A. DWIA calculations

The analysis described here follows closely that reported in Refs. [42] and [26] and more details can be found there. The distorted-wave impulse-approximation (DWIA) calculations used the codes ALLWRLD [43] and MSUDWPI [44] with the spin-orbit force and optical potential parameters similar to those reported previously, and a charge radius of 3.24 fm determined from electron scattering [45]. The ground-state density distribution parameters used for both protons and neutrons in these two codes were taken to have a Woods-Saxon form with radius $c=3.08$ fm and diffuseness $a=0.55$ fm. These values were determined as in Ref. [26]. If instead, older values of $c=3.458$ fm, $z=0.6098$ fm, and $w=-0.208$ are used [46], the theoretical pion-scattering calculations decrease by about 8%.

The transition density input for ALLWRLD used pion-scattering parameters fixed at the values that best fit the stretched state electron scattering data. The set with simple harmonic oscillator (HO) single nucleon wave functions used $b=1.80 \pm 0.04$ fm [3]. The set with Woods-Saxon (WS) wave functions (which are especially important for unbound states) used $r_0=1.26 \pm 0.03$ fm and diffuseness and spin-orbit parameters of $a=0.65$ fm and $\lambda=25$, respectively.

The WS wave functions were calculated using the code DWUCK4 [47]. The binding energy (BE) for the proton and neutron wave functions used their respective separation energies. The binding energy for a given excited state equaled its excitation energy (EE) minus the nucleon separation energy (SE) for ^{32}S and the energy of the lowest $5/2^+$ state in the mass 31 nuclei ($\text{BE} = \text{EE} - \text{SE} - E_{5/2}$). The neutron and proton separation energies for ^{32}S are 15.04 and 8.86 MeV, respectively. The lowest $5/2^+$ state, taken as the hole for the stretched excitation, is located at 2.24 MeV for ^{31}S and 2.23 MeV for ^{31}P . Thus, states below 11.09 MeV have both the neutron and proton bound and the remainder up to 17.28 MeV have the neutron bound and proton unbound.

The WS wave functions for the ^{32}S electron-scattering theory calculations in Ref. [3] used a nonlocal parameter (PNLOC) equal to 0.85. In that case, $r_0=1.20 \pm 0.04$ fm was needed for a best fit to the stretched state electron-scattering data and the total Z_1^2 (independent of pion data) was 88%. In

TABLE IV. Values used to calculate the structure coefficients in ^{32}S . The experimental cross sections for pion scattering at the top of the angular distribution are from a least-squares fit to the data. (The listed values are an average between HO and WS fits, with the actual values well within the uncertainties given.) The theoretical DWIA pion cross sections, $(M_1^\pi)^2$, at the peak of the angular distribution were calculated using ALLWRLD and MSUDWPI. The experimental form factors, F^2 , for electron scattering from Ref. [3] were determined in a similar fashion and are also listed. The theoretical electron cross section, $(M_1^e)^2$, at the peak of the angular distribution, is 25.7×10^{-5} for HO wave functions and is listed for the WS wave functions. None of the calculations included MEC effects.

E_x (MeV)	HO				WS		F^2 $\times 10^{-5}$	WS $(M_1^e)^2$ $\times 10^{-5}$
	σ^- ($\mu\text{b/sr}$)	σ^+ ($\mu\text{b/sr}$)	$(M_1^+)^2$ ($\mu\text{b/sr}$)	$(M_1^-)^2$ ($\mu\text{b/sr}$)	$(M_1^+)^2$ ($\mu\text{b/sr}$)	$(M_1^-)^2$ ($\mu\text{b/sr}$)		
9.7	4.0 ± 1.9	9.3 ± 1.3	62.5	54.7	54.2	61.3		
10.9	7.6 ± 1.5	6.6 ± 1.7	61.6	53.8	54.3	61.0		
11.0	2.5 ± 0.7	3.1 ± 0.6	61.5	53.7	54.3	61.0	3.4 ± 0.2	24.4
11.2							0.8 ± 0.1	24.3
11.9	4.4 ± 0.2	4.4 ± 0.5	60.8	53.0	54.4	60.5	3.2 ± 0.3	23.8
12.6	3.4 ± 0.8	14.6 ± 2.8	60.3	52.6	54.5	59.9		
12.7	12.2 ± 2.9	8.4 ± 2.0	60.2	52.5	54.5	59.7	3.1 ± 0.1	23.1
13.3	< 2	< 2	59.8	52.1	54.7	59.0	0.9 ± 0.1	22.7
13.5	3.1 ± 3.0	8.3 ± 1.7	59.6	51.9	54.8	58.6	2.2 ± 0.3	22.4
14.3	3.9 ± 1.3	3.0 ± 0.3	59.0	51.4	54.9	57.3	1.5 ± 0.1	21.6
16.4	3.5 ± 1.3	3.1 ± 1.3	57.5	50.0	54.1	55.6	1.5 ± 0.1	19.4
16.6	5.8 ± 1.6	6.2 ± 0.6	57.3	49.8	53.3	56.8		
17.1	4.3 ± 0.7	5.7 ± 0.8	56.9	49.4	50.1	64.7	1.5 ± 0.1	19.3

this paper a PNLOC of zero was used, giving a total Z_1^2 (independent of pion data) of 78%.

B. Structure coefficient calculations

The differential cross section for pion scattering to stretched magnetic transitions can be written schematically as

$$\sigma^\pm = N f_{\text{c.m.}}^2 (M_1^\pm)^2 \left[\frac{M_0^\pm}{M_1^\pm} Z_0 + Z_1 \right]^2, \quad (1)$$

where N (assumed here to be equal for π^+ and π^-) is an empirical normalization of the pion calculated cross sections to known isovector electron scattering strengths, M_τ^\pm are matrix elements calculated in the DWIA, and Z_τ are spectroscopic structure coefficients for a pure isoscalar ($\tau=0$) or isovector ($\tau=1$) single particle-hole 6^- transition. For incident pion energies near the $\Delta_{3,3}$ resonance, $M_0^\pm/M_1^\pm \approx \mp 2$ for π^\pm scattering. The standard center-of-mass correction was made by reducing the HO b or the WS r_0 derived from electron scattering by $[(A-1)/A]^{1/2}$, before using it for the (π, π') DWIA calculations. The final theoretical cross sections were then increased by $f_{\text{c.m.}}^2 = [A/(A-1)]^L$ which equals 1.17 for ^{32}S , $L=5$ transitions. The simplifying characteristics of stretched excitations which justify the form of Eq. (1) have been discussed elsewhere [1].

A similar equation can be written for electron scattering form factors in order to compare pion and electron scattering data:

$$F^2 = (M_1^e)^2 \left[\frac{M_0^e}{M_1^e} Z_0 + Z_1 \right]^2, \quad (2)$$

where nucleon finite size and center-of-mass factors are contained in the isoscalar and isovector electromagnetic matrix elements M_0^e and M_1^e . Distorted-wave Born approximation effects are included in the standard q_{eff} approximation.

The magnitude of the calculated DWIA pion angular distribution was varied to fit the data for each ^{32}S 6^- state until a best χ^2 fit was obtained as shown in Figs. 3 to 5. Note that the theoretical HO and WS curves are about the same for π^- , whereas, for π^+ the WS curve peaks at a smaller angle than the HO, resulting in a worse WS fit. The resulting σ^\pm cross sections at the peak of the form factor as used in Eq. (1) are listed in Table IV. For electron scattering, the F^2 used in Eq. (2) were determined by a similar procedure and are also listed in Table IV.

The $(M_1^\pm)^2$ [$= \sigma_{1DW}^\pm$ for $Z_0=0$ and $Z_1=1$] cross sections were calculated by ALLWRLD and MSUDWPI using both HO and WS wave functions, and the $(M_1^e)^2$ were calculated with a simple electron scattering code. Results are given in Table IV. The $|M_0^\pi/M_1^\pi|$ ratio used in Eq. (1) for 162 MeV pion scattering was determined from ALLWRLD and MSUDWPI to be 1.93 for HO wave functions. With WS wave functions, this ratio was approximately -1.8 for π^+ and 2.0 for π^- , varying only slightly with excitation energy. The M_0^e/M_1^e ratio used in Eq. (2) for electron scattering was -0.187 for HO wave functions and varied from -0.11 to -0.17 for WS wave functions, depending upon the excitation energy.

For excited states where the electron and both pion scattering cross sections were known, the *ratio method* was used for calculating the Z coefficients. In this method, the Z_0/Z_1 ratio is relatively model independent and is determined mainly by the well-known M_0^π/M_1^π ratio near $\Delta_{3,3}$ resonance energies. Eq. (1) was solved to give the ratio

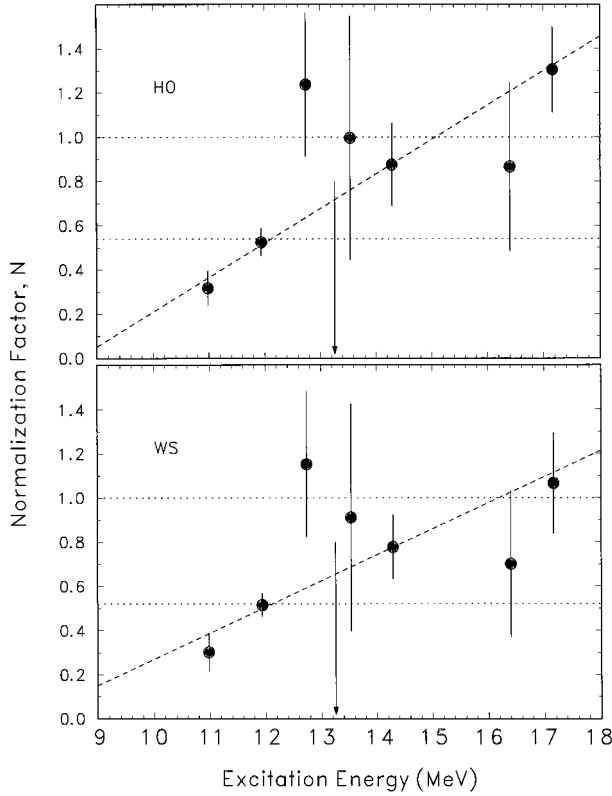


FIG. 8. Normalization factors determined for each state from the HO and WS calculations. The horizontal lines are at unity and at the average normalizations of 0.54 for HO and 0.52 for WS. The diagonal lines represent a least squares fit of $N=0.16E-1.35$ for HO and $N=0.12E-0.91$ for WS.

$$\frac{Z_0}{Z_1} = -\frac{M_1^+ \pm M_1^- \sqrt{R}}{M_0^+ \pm M_0^- \sqrt{R}}, \quad (3)$$

where $R = \sigma^+ / \sigma^-$. Using this Z_0/Z_1 ratio and Eq. (2), both Z_0 and Z_1 were calculated. The normalization N necessary for the DWIA calculations was then determined from Eq. (1) and these factors with their uncertainties are plotted for each state in Fig. 8. An ideal normalization of unity would signify that no adjustment of the pion DWIA calculations was necessary to arrive at agreement with electron-scattering data.

For the excited states where no electron-scattering data were available, the *absolute method* was used instead. In this case, a normalization had to be assumed in order to calculate the two Z coefficients from Eq. (1). This assumed normalization is very model dependent and several different methods for determining it were compared.

C. The structure coefficients and normalization factors

The Z structure coefficients calculated in the *ratio method* are somewhat dependent on electron model calculations. The Z_1 values are determined from electron-scattering data and are inversely proportional to any variation in M_1 from the electron scattering theory calculations. The Z_0 values are determined from pion-scattering data, but are relatively independent of the pion theory calculations, because they are determined relative to Z_1 from the well-known π^+/π^- ratio near resonance. Only the normalization N is affected by the

pion theory calculations. Thus, the Z_0 and Z_1 coefficients are affected in a similar fashion by any change in (e, e') calculations, but are mostly independent of any change in (π, π') calculations.

The use of WS instead of HO wave functions in the electron scattering analysis decreases the theoretical cross sections by 5 to 33 % as seen in Table IV, which would increase the Z^2 coefficients by similar factors. If isovector meson exchange current (MEC) contributions were included in the electron-scattering calculations [48], the theoretical cross sections would be 15 to 17 % larger, thus reducing the value of each of the Z^2 coefficients by the same amount.

The Z coefficients calculated in the *absolute method* are very dependent on pion model calculations, because of uncertainties in the normalization N . A comparison of Z coefficients using several different normalization factors is shown in Table V for the possible new isoscalar 6^- states. The normalization factors are: (i) a constant N of 1.28 equal to the average from the other sd -shell nuclei, ^{24}Mg , ^{26}Mg , and ^{28}Si [9,20,26]; (ii) a constant N of unity, meaning that no adjustment was made to the DWIA pion scattering calculations; (iii) a constant $N=0.54$ which is the average from the *ratio method* using HO wave functions; (iv) a variable N based on the linear least squares fit to the HO normalization factors of the states found in electron scattering; and (v) an N from a nearby 6^- stretched state observed in electron scattering. A weighted mean of the N from (ii) through (v) is also shown. The Z coefficients from this weighted mean are used in further calculations and the uncertainties given for Z include the systematic uncertainties in the normalization N .

In addition to the variation in N and Z shown in Table V, the theoretical pion-scattering calculations were varied to give a different $(M_1^\pi)^2$ by using the ground-state change density distribution from Ref. [46]. This change decreased the theory calculations by 8%, which would result in a corresponding increase of 8% in either the normalization or the Z^2 values, but not both.

The Z coefficients as calculated above are tabulated in Table VI and the Z^2 values are compared to (p, n) results and to theory in Table VII. The sums of the squares of the Z coefficients are tabulated in Table VIII. These experimental structure coefficients can in the first approximation be compared to the extreme-single-particle-hole-model (ESPHM) sum rules given in Ref. [14]. The total structure coefficients for ^{32}S should add to $\sum Z_0^2 = \sum Z_1^2 = 1$. In a more complete analysis the experimental structure coefficients can be compared to LBSM calculations [28]. Both of these theoretical results are shown in Table VIII, along with the experiment-to-theory ratios.

V. DISCUSSION

A. Pion DWIA normalization

Previous experiments have found that the M_7^\pm pion-scattering matrix elements calculated with the DWIA model and used in Eq. (1) usually require an empirical normalization factor N to reproduce the isovector spectroscopic coefficients Z_1 calculated from electron scattering [26,9,20]. This normalization factor can only be calculated for stretched

TABLE V. A tabulation of various HO Z coefficients for possible new isoscalar ^{32}S 6^- stretched states. Normalization factors used in this table are (i) an average N from other sd -shell nuclei, (ii) an N equal to unity, (iii) an average N from the ^{32}S isovector states, (iv) a variable $N=0.16E-1.35$, and (v) an N from a nearby 6^- state. A weighted mean from (ii)–(v) is shown and the resulting Z coefficients are used in further calculations. See text for more details.

E_x (MeV)	N	Z_0	Z_1	source for N
9.65	1.28 ± 0.07	-0.14 ± 0.02	0.06 ± 0.03	^{24}Mg , ^{26}Mg , ^{28}Si average
	1.00 ± 0.15	-0.16 ± 0.02	0.07 ± 0.04	unity
	0.54 ± 0.11	-0.22 ± 0.03	0.10 ± 0.05	^{32}S average
	0.15 ± 0.45	-0.41 ± 0.43	0.18 ± 0.84	linear variation no nearby 6^- state
	$\bar{N}=0.68 \pm 0.16$	-0.19 ± 0.03	0.09 ± 0.05	mean
10.88	1.28 ± 0.07	0.15 ± 0.01	0.01 ± 0.02	^{24}Mg , ^{26}Mg , ^{28}Si average
	1.00 ± 0.15	0.16 ± 0.02	0.01 ± 0.03	unity
	0.54 ± 0.11	0.22 ± 0.03	0.01 ± 0.05	^{32}S average
	0.34 ± 0.47	0.28 ± 0.14	0.01 ± 0.26	linear variation
	0.32 ± 0.08	0.29 ± 0.04	0.01 ± 0.07	10.98 MeV state
$\bar{N}=0.48 \pm 0.13$	0.24 ± 0.03	0.01 ± 0.06	mean	
12.63	1.28 ± 0.07	-0.16 ± 0.01	0.11 ± 0.03	^{24}Mg , ^{26}Mg , ^{28}Si average
	1.00 ± 0.15	-0.18 ± 0.02	0.13 ± 0.03	unity
	0.54 ± 0.11	-0.24 ± 0.03	0.17 ± 0.05	^{32}S average
	0.62 ± 0.50	-0.23 ± 0.07	0.16 ± 0.14	linear variation
	1.24 ± 0.33	-0.16 ± 0.02	0.11 ± 0.04	12.74 MeV stat
$\bar{N}=0.73 \pm 0.15$	-0.21 ± 0.02	0.15 ± 0.05	mean	
16.65	1.28 ± 0.07	-0.14 ± 0.01	0.01 ± 0.02	^{24}Mg , ^{26}Mg , ^{28}Si average
	1.00 ± 0.15	-0.16 ± 0.01	0.01 ± 0.03	unity
	0.54 ± 0.11	-0.21 ± 0.02	0.02 ± 0.04	^{32}S average
	1.24 ± 0.59	-0.14 ± 0.03	0.01 ± 0.05	linear variation
	0.87 ± 0.38	-0.17 ± 0.03	0.01 ± 0.06	16.4 MeV state
$\bar{N}=0.72 \pm 0.16$	-0.18 ± 0.02	0.01 ± 0.04	mean	

states where data are available for all three of electron, π^+ , and π^- scattering reactions. This severely limits the number of states available for comparison.

Normalization factors vary considerably from nucleus to nucleus: 1.0 for ^{28}Si , 1.2 to 1.4 (depending on incident pion energy and the use of HO or WS wave functions) for $^{24,26}\text{Mg}$, 2 for ^{54}Fe , and 5 for ^{60}Ni . A value larger than unity signifies that the pion cross sections are larger than expected from the electron-scattering data. In contrast to these, the average normalization N for ^{32}S stretched states is less than unity—0.54 when using HO wave functions and 0.52 with WS. The pion-scattering cross sections were in general smaller than expected from the electron-scattering data, and the necessary normalization was smaller than for any of the other nuclei studied previously.

Normalization factors also vary significantly between states within a given nucleus: 1 to 2 for ^{26}Mg , 1 to 4 for ^{54}Fe , and 4 to 8 for ^{60}Ni [26,20]. The variation could perhaps be explained by the fact that these nuclei are not self-conjugate and these states have mixed isoscalar and isovector components. In looking for a trend in the variation, the correlation between normalization and excitation energy (in MeV) was calculated as 0.07 ± 0.08 for ^{26}Mg , 0.21 ± 0.23 for ^{54}Fe , and -0.15 ± 0.24 for ^{60}Ni . A slight positive trend may

be possible, but it is not significantly different from zero.

The seven states in ^{32}S significantly increase the possibilities for studying the variation in normalization between different states in a given nucleus. This is the first nucleus in which several supposedly pure isovector stretched transitions have been observed in a single nucleus, and where the stretched states should not have mixed isoscalar and isovector components. Theoretically, the relative sizes of the isovector ^{32}S peaks should be the same in pion and electron-scattering spectra, independent of uncertainties in pion DWIA theory. This was definitely not the case experimentally, where the normalization factor for the several isovector states varied from 0.4 to 1.4, as seen in the upper part of Fig. 8. The three strongest states observed in electron scattering were located at 11.0, 11.9, and 12.7 MeV and were approximately equal in size. In contrast, the pion spectra in Fig. 1 show a strong state at 12.7 MeV, with much weaker states at 11.0 and 11.9 MeV (see also Table IV). Although the two weaker states could not be separated from nearby strong states of lower multipolarity, there are obviously no states at excitation energies of 11.0 and 11.9 MeV as strong as the state at 12.7 MeV. For these states, the (π, π') data are in better agreement with the (p, n) data and the LBSM predictions than with the (e, e') data. The resulting normalization

TABLE VI. A tabulation of Z coefficients for ^{32}S 6^- stretched states extracted from a combined analysis of electron- and pion-scattering data. Both HO and WS wave functions were used and no MEC effects have been included. The Z_1 coefficients have arbitrarily been chosen to be the positive solution. The *ratio method* was used to calculate Z coefficients except for those marked with an asterisk, in which case the *absolute method* was used. The N used in the calculations is shown. The small Z coefficients compatible with zero are not included in the Table VII tabulation.

E_x (MeV)	HO			WS		
	N	Z_0	Z_1	N	Z_0	Z_1
*9.7	0.68 ± 0.16	-0.19 ± 0.03	0.09 ± 0.05	0.64 ± 0.16	-0.20 ± 0.03	0.09 ± 0.05
*10.9	0.48 ± 0.13	0.24 ± 0.03	0.01 ± 0.06	0.49 ± 0.14	-0.24 ± 0.03	0.00 ± 0.06
11.0	0.32 ± 0.08	-0.02 ± 0.02	0.36 ± 0.01	0.30 ± 0.09	-0.01 ± 0.02	0.37 ± 0.01
11.2		0.00 ± 0.00	0.17 ± 0.01		0.00 ± 0.00	0.17 ± 0.01
11.9	0.52 ± 0.06	-0.01 ± 0.01	0.35 ± 0.01	0.52 ± 0.05	0.00 ± 0.01	0.36 ± 0.02
*12.6	0.73 ± 0.15	-0.21 ± 0.02	0.15 ± 0.05	0.67 ± 0.15	-0.22 ± 0.02	0.16 ± 0.05
12.7	1.24 ± 0.33	0.01 ± 0.01	0.35 ± 0.01	1.15 ± 0.33	0.02 ± 0.02	0.37 ± 0.01
13.3	< 0.8	0.00 ± 0.02	0.19 ± 0.01	< 0.8	0.00 ± 0.02	0.20 ± 0.01
13.5	1.00 ± 0.55	-0.04 ± 0.05	0.29 ± 0.02	0.91 ± 0.51	-0.04 ± 0.05	0.30 ± 0.02
14.3	0.88 ± 0.19	0.01 ± 0.01	0.24 ± 0.01	0.78 ± 0.15	0.01 ± 0.01	0.26 ± 0.01
16.4	0.87 ± 0.38	0.00 ± 0.02	0.24 ± 0.01	0.70 ± 0.33	0.00 ± 0.02	0.27 ± 0.01
*16.6	0.72 ± 0.16	0.18 ± 0.02	0.01 ± 0.04	0.66 ± 0.15	-0.20 ± 0.02	0.02 ± 0.04
17.1	1.31 ± 0.19	-0.01 ± 0.01	0.24 ± 0.01	1.07 ± 0.23	0.00 ± 0.01	0.27 ± 0.02
$\Sigma Z_\tau^2 =$		0.17 ± 0.02	0.73 ± 0.03		0.19 ± 0.02	0.82 ± 0.03

of the DWIA calculations as shown in Fig. 8 requires $N=1.2$ for the 12.7 MeV state, but $N=0.3$ and 0.5 for the two weak states. This figure shows a general trend of increasing normalization with excitation energy giving a positive correlation of 0.16 ± 0.03 . The correlation would be almost perfect if the states at 12.74 and 16.4 MeV that were

identified as part of isospin pairs were ignored. If the strengths of the pion-scattering transitions are instead compared to those extracted from the (p,n) data, the trend of increasing normalization with excitation energy is less pronounced, but still present. However, if we ignore the 11.0 and 11.9 MeV states that are comparatively weak in the

TABLE VII. Structure coefficients are listed for the ^{32}S 6^- transitions derived from our combined electron-pion analysis, where HO wave functions were used and no MEC effects were included. For comparison, spectroscopic strengths from the $^{32}\text{S}(p,n)^{32}\text{Cl}$ reaction [4] and theoretical predictions from LBSM calculations [28,36] are listed.

E_x (MeV)	$(e,e') + (\pi,\pi')$		$^{32}\text{S}(p,n)$		^{32}S theory		
	Z_0^2	Z_1^2	E_x (MeV)	S^2	E_x (MeV)	Z_0^2	Z_1^2
9.7	0.037	0.008			8.54	0.011	
					9.21	0.028	
					10.36	0.152	
10.9	0.056			10.94	0.039		
11.0		0.132	3.8	0.068	11.29		0.042
11.2		0.030					
11.9		0.124	4.7	0.077	11.84		0.007
12.6	0.043	0.022					
12.7		0.122	5.6	0.119	12.74		0.302
13.3		0.036	6.3	0.102			
13.5		0.082	6.8	0.034	13.42		0.033
14.3		0.058	7.4	0.047			
			8.4	0.013			
16.4		0.060	9.2	0.038			
16.6	0.034						
17.1		0.058	9.8	0.051			
$\Sigma Z_\tau^2 =$		0.172		0.549		0.230	0.374

TABLE VIII. Listed here are the sums of the experimental Z^2 coefficients derived from a combined electron-pion analysis for the 6^- states in ^{32}S , compared to results from a similar analysis on other self-conjugate sd -shell nuclei [28]. Harmonic oscillator wave functions were used with no MEC effects included. The theoretical Z coefficients are from the ESPHM sum rules of Ref. [14] and from the LBSM calculations of Ref. [28]. The 1Δ are the sum over discrete theoretical isovector states and the $1f$ is the sum of predicted isovector strength over the 6–8 MeV region of excitation energy where the experimental strength has been observed. The ratio between experiment and theory is defined as $S_\tau^2 = \Sigma(Z_\tau^2)_{\text{exp}} / \Sigma(Z_\tau^2)_{\text{th}}$.

	τ	ESPHM			τ	LBSM	
		$\Sigma(Z_\tau^2)_{\text{exp}}$	$\Sigma(Z_\tau^2)_{\text{th}}$	S_τ^2		$\Sigma(Z_\tau^2)_{\text{th}}$	S_τ^2
^{20}Ne	0		1/3		0	0.16	
	1	0.03	1/3	0.10	1Δ	0.18	0.19
^{24}Mg					$1f$	0.18	0.19
	0	0.05	2/3	0.07	0	0.20	0.25
	1	0.19	2/3	0.29	1Δ	0.32	0.59
^{28}Si					$1f$	0.37	0.51
	0	0.13	1	0.13	0	0.20	0.65
	1	0.29	1	0.29	1Δ	0.37	0.78
^{32}S					$1f$	0.70	0.41
	0	0.17	1	0.17	0	0.23	0.75
	1	0.73	1	0.73	1Δ	0.38	1.92
					$1f$	0.77	0.95

(p, n) reaction as they are in this (π, π') reaction, the normalization would be approximately constant at unity.

One explanation for the variation in N is a varying fragmentation of strength due to isospin mixing. Another possibility is that N increases with excitation energy due to the unbound nature of the nucleons. This effect is included in the theoretical calculations by the use of unbound WS wave functions. The resulting WS normalization factors are shown in the lower part of Fig. 8 and the correlation between N and excitation energy is calculated as 0.12 ± 0.03 . This correlation is closer to zero than with HO wave functions, showing that the use of unbound WS wave functions is an improvement in the theory.

B. Quenching

It has been generally observed that the total spectroscopic strength for known stretched transitions is significantly less than the maximum allowed by the ESPHM [1,2,48], with the isoscalar component affected a factor of 2 or 3 more strongly than the isovector [1,24,26]. Attempts have been made to reproduce this experimental quenching, e.g., by using a larger basis model [49] and by using a deformed model [50]. The even greater quenching of isoscalar strength with respect to isovector has been attributed to differences in the structure of the two types of transition densities [51,52]. The inclusion of MEC effects increases the disagreement between theory and experiment [48], although the use of unbound WS wave functions instead of the usual HO wave functions offsets this increase in some cases [42]. Proper inclusion of these continuum effects is an important open problem [28] and the use of cross-section ratios to determine spectroscopic amplitudes

for unbound states must be done with care [53]. Theoretical predictions for the structure and isospin mixing, and therefore the pion cross sections, of the unbound stretched states in ^{12}C are significantly affected when recoil-corrected continuum shell-model calculations are done [54].

For the previously studied ^{24}Mg and ^{28}Si self-conjugate sd -shell nuclei, 29% of the isovector $M6$ ESPHM strength is exhausted by the electron-scattering data (see Table VIII). More realistic RPA calculations including ground state correlations predict a summed strength about half that of ESPHM calculations [55], but still the experimental strengths for these two nuclei are only about half the RPA predictions [8,23]. More recently, the use of LBSM calculations have found that the experimental isovector strengths exhaust 59% and 78% of theory for ^{24}Mg and ^{28}Si respectively [28], and 79% for the ^{26}Mg nucleus [20,56].

The total isovector strength for 6^- stretched states in ^{32}S , as determined from electron-scattering data [3], is found to exhaust 71% of the ESPHM isovector strength. This large fraction in ^{32}S is related to the fact that the $d_{5/2}$ orbit has a greater ground state occupancy in this nucleus than in the lower mass sd -shell nuclei [57]. With LBSM calculations, the data exhaust 95% of the sum of the predicted isovector strength over the 6–8 MeV region where states have been experimentally observed [58,28]. These observations about the isovector states are from electron scattering and are little affected by the pion data.

The total isoscalar strength for ^{32}S is only 17% of that predicted by the ESPHM sum rule when using the mean normalization shown in Table V. This changes to 8% when the average normalization of $N=1.28$ from the other self-

conjugate sd -shell nuclei is used for all states, to 11% when a normalization of unity is used, to 20% when the average ^{32}S normalization of $N=0.54$ is used, and to 31% when a linearly varying normalization (with large uncertainties) for each state is used. If the ground-state charge distribution from Ref. [46] is used this changes to 19%, and if WS wave functions are used it becomes 19%. We conclude that the isoscalar strength exhausts approximately $17 \pm 6\%$ of the ES-PHM sum rule, if the four tentative new isoscalar states are in fact 6^- states. This fraction of isoscalar strength observed in ^{32}S is greater than the 7 to 13% for the other sd -shell nuclei, although not as great as that for the ^{12}C and ^{16}O p -shell nuclei [26].

The use of LBSM calculations better reproduces the quenching of the isoscalar strength in ^{32}S , with the experimental data (including the questionable cases) exhausting $75 \pm 26\%$ of the calculations. This is a significant improvement over the 65% for ^{28}Si , 25% for ^{24}Mg , and 23% for ^{26}Mg [20].

C. Fragmentation

Previously, only asymmetric $T_0 \neq 0$ nuclei were found to exhibit much fragmentation of the stretched transitions, viz., ^{14}C and ^{26}Mg for isoscalar transitions [15,20] and ^{58}Ni and ^{60}Ni for isovector transitions as well [59,27]. Coherent mixtures of isoscalar and isovector strengths are allowed between the states in these nuclei due to their neutron excess and the stretched strength is fragmented among a number of states. The non-self-conjugate ^{30}Si nucleus is a similar case, but the incomplete electron-scattering data for 6^- stretched states have only partially been analyzed [60].

In self-conjugate nuclei, any 6^- stretched excitation is expected to be either purely isoscalar or purely isovector. The RPA calculations predict only one strong $M6$ isovector excitation in self-conjugate sd -shell nuclei from ^{20}Ne to ^{40}Ca [55]. Similarly, LBSM calculations predict one strong isovector state and one strong isoscalar state for each self-conjugate sd -shell nucleus from ^{20}Ne to ^{32}S , although several are expected for ^{36}Ar [28]. Experimental work on ^{24}Mg and ^{28}Si has found one such strong isovector 6^- state by electron scattering on each nucleus [8,5], and one isoscalar 6^- state each by pion scattering [9,22]. In the p -shell nuclei, one strong isovector state each has been observed by electron scattering in the ^{12}C and ^{16}O self-conjugate nuclei [13,19]. These can be compared to calculations done for $M4$ excitations in p -shell nuclei [61].

It should be noted in passing that a second weak isovector 6^- state has recently been reported from $^{28}\text{Si}(e,e')$ [62] and several additional weak 6^- candidates have been identified using polarized proton scattering [63]. Also, in the final state nuclei corresponding to $^{20}\text{Ne}(p,n)$, $^{24}\text{Mg}(p,n)$, and $^{28}\text{Si}(p,n)$ the 6^- strength was fragmented between several states [4].

The ^{32}S nucleus is unique in being the first self-conjugate nucleus where the isovector strength is not concentrated in a single 6^- state [3]. Increased fragmentation in passing from ^{28}Si to ^{32}S has similarly been found for the $M1$ strength [64]. The fragmentation of $M6$ strength in ^{32}S is in contrast with the systematics for isovector $M4$ transitions in the p shell, where the 4^- strength is concentrated in one state for

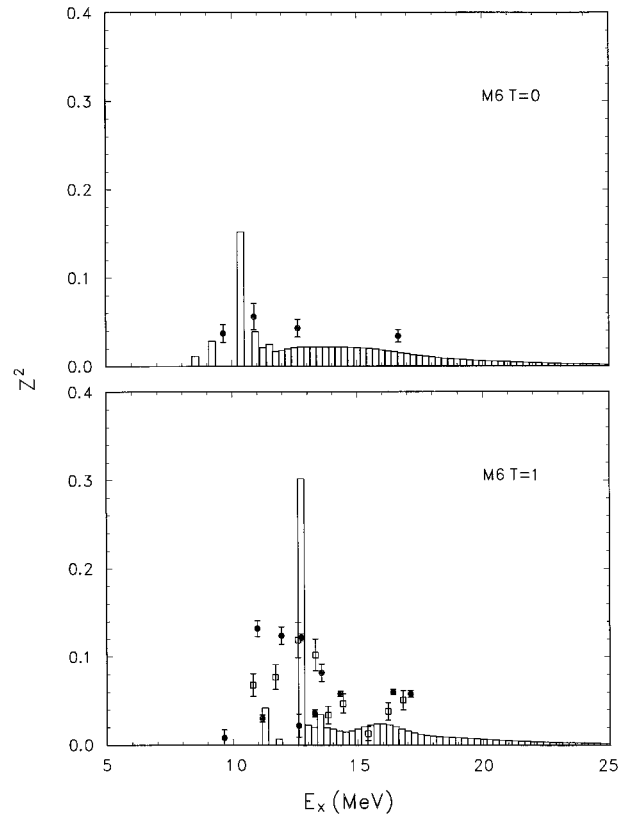


FIG. 9. The HO Z^2 coefficients from Table VII for ^{32}S 6^- stretched states are plotted as solid circles. The error bars show the experimental uncertainties, but do not include the variety of theoretical uncertainties. For comparison, the S^2 coefficients from the (p,n) reaction [4] are plotted as open rectangles. The histograms display the predicted strength for these stretched states as obtained with the $n_{\text{max}}=8$ basis [28,36].

^{16}O . Apparently, the four $2s_{1/2}$ spectator nucleons in ^{32}S (beyond ^{28}Si) play a different role than the four $p_{1/2}$ spectator nucleons in ^{16}O (beyond ^{12}C). The fragmentation of 6^- strength in ^{32}S may be due to having the stretched transitions built on several $d_{5/2}$ hole states other than the ground state. Using nucleon pick-up reactions, several strong $d_{5/2}$ hole states were found for ^{32}S , but only one strong $d_{5/2}$ hole state was found for ^{24}Mg and ^{28}Si [65], and only one strong $p_{3/2}$ hole state was found for ^{16}O [66]. The LBSM calculations show fragmentation among several states of approximately equal strength in ^{36}Ar , but apparently this expectation is first realized in the lower mass ^{32}S nucleus.

This experiment extends the data on ^{32}S 6^- fragmentation to isoscalar states. From LBSM calculations, the isoscalar strength was expected to be concentrated in one state; however, both isoscalar and isovector strength was expected near 11 MeV of excitation, suggesting that the strength would actually be isospin mixed [58]. Experimentally, the isoscalar strength is fragmented between several tentative new isoscalar states in this energy region. They are close in excitation energy to previously observed isovector states and in at least one case at 12.6/12.7 MeV are isospin mixed with them. In addition, there is probably isospin mixing in the 16.4 MeV region. The upper part of Fig. 9 summarizes

the experimental and predicted ^{32}S 6^- isoscalar strength in the energy range between 9 and 18 MeV [28,36], and the lower part of Fig. 9 shows the distributions of isovector strength.

D. Asymmetries

Pion-scattering to pure isoscalar or isovector states, as found in self-conjugate nuclei, would normally expect to find equal cross sections for π^+ and π^- , except for the fact that neutrons and protons generally have different binding energies. The ability of the pion to probe neutrons and protons separately should demonstrate the asymmetry of π^+ and π^- results when exciting stretched transitions where the proton is bound and the neutron is unbound. In addition to the usual HO wave functions, more realistic WS wave functions with unbound states treated as resonances are useful in analyzing these cases [42].

Experimentally, pion-scattering to stretched states that were expected to be purely isovector or purely isoscalar has often found σ^-/σ^+ ratios unequal to unity. For the stretched states in ^{12}C , enhancement of π^- over π^+ scattering due to nucleon binding asymmetries has been predicted [67], but is not sufficient to explain the data [12]. The cross-section asymmetry in ^{16}O apparently cannot be explained by binding energy asymmetries either, even though the excitation energies of its stretched states are close to where the proton becomes unbound [18]. For these two nuclei, the unequal π^- and π^+ cross sections for most of the stretched transitions have instead been explained by isospin mixing. For the $T=1$ state in ^{28}Si , the σ^-/σ^+ ratio is smaller than unity and difficult to understand, but the π^- data are sparse [68]. The larger than unity σ^-/σ^+ ratio for the 13.9 MeV $T=3$ stretched state in ^{60}Ni can be attributed to having the proton unbound for this state and the neutron bound. Unbound WS wave functions were partly able to reproduce this effect [26].

In ^{32}S the proton separation energy of 9 MeV is much less than the neutron separation energy of 15 MeV. This difference is greater than that in previously studied self-conjugate nuclei, making it a good case to study binding energy asymmetry. Overall, the total σ^- cross section of $55 \pm 6 \mu\text{b/sr}$ is significantly less than the total σ^+ cross section of $73 \pm 5 \mu\text{b/sr}$. More specifically, Table IV shows four individual states that have unequal cross sections for π^- and π^+ that are at or beyond their experimental uncertainties, with $\sigma^- < \sigma^+$ in each case. Isospin mixing explains the asymmetry of the 12.6/12.7 MeV pair, but there are three additional states at 9.7, 13.5, and 17.1 MeV. This general trend of a σ^-/σ^+ ratio smaller than unity corresponds to the $(M_1^+)^2/(M_1^-)^2$ ratio smaller than unity obtained from the use of unbound WS wave functions shown in the same table.

VI. CONCLUSIONS

This pion-scattering work has complemented (e, e') and (p, n) studies to provide the isovector and isoscalar strengths to fragmented 6^- stretched states in ^{32}S , including several

possible new 6^- isoscalar states first observed in these pion-scattering data.

The normalization of the pion theory calculations needed to reproduce the isovector spectroscopic coefficients from electron scattering was less than unity and significantly smaller than for previous sd -shell nuclei, with a trend of increasing normalization with larger excitation energy. The trend is less pronounced, but still present, when the strengths of the pion-scattering transitions are compared to those extracted from the (p, n) data. Model dependence of the normalization factor results in large uncertainties when calculating the structure coefficients for the isoscalar states.

The summed strengths for ^{32}S isovector transitions (determined primarily from electron scattering) are stronger than in other sd -shell nuclei and are approximately equal to theoretical calculations, if all our assignments are valid. The strength of isoscalar transitions shows the same pattern as noted in other nuclei of being quenched below theoretical values; however, the isoscalar strength is larger than the fraction found for any other sd -shell nucleus and comes close to that predicted by LBSM calculations, if the possible new isoscalar states are included and if a normalization of less than unity is used. This pion-scattering experiment on ^{32}S is an important complement to electron scattering in studying the trend of small isoscalar/isovector strength ratios. An improved $^{32}\text{S}(p, p')$ experiment with better energy resolution needs yet to be done on this nucleus to confirm the 6^- assignments.

The fragmentation of the isovector strength in ^{32}S as observed in electron scattering was found to extend to the isoscalar strength as well. This nucleus is unique in being the first self-conjugate nucleus where neither the isovector nor the isoscalar stretched strength is concentrated in a single state.

The use of unbound Woods-Saxon wave functions, instead of those from an harmonic oscillator potential, resulted in slightly better agreement between data and theory for several features. (i) The WS wave functions were partly able to reproduce the trend of increasing normalization with larger excitation energy. (ii) The inclusion of asymmetric nucleon binding energies by the use of WS wave functions resulted in better agreement with the general feature of $\sigma^- < \sigma^+$ cross section. (iii) The use of WS wave functions gave a moderately increased magnetic strength. There is some question about the proper inclusion of unbound effects, so we have emphasized the use of HO wave functions throughout this paper as a better standard for comparison with previous work; however, the results reported here suggest that more study on the use of unbound wave functions would be beneficial in explaining the experimental data.

ACKNOWLEDGMENTS

This work was supported in part by the National Science Foundation and the U. S. Department of Energy, including support through the Associated Western Universities. We would also like to thank Enoch Hwang and Denny Lin at the La Sierra University computer center for the use of the facilities.

- [1] R. A. Lindgren and F. Petrovich, in *Spin Excitations in Nuclei*, edited by F. Petrovich *et al.* (Plenum, New York, 1984), p. 323; R. A. Lindgren, J. Phys. (France) Colloq. **45**, 433 (1984).
- [2] F. Petrovich, J. A. Carr, and H. McManus, Annu. Rev. Nucl. Part. Sci. **36**, 29 (1986).
- [3] B. L. Clausen, R. A. Lindgren, M. Farkhondeh, L. W. Fagg, D. I. Sober, C. W. de Jager, H. de Vries, N. Kalantar-Nayestanaki, B. L. Berman, K. S. Dhuga, J. A. Carr, F. Petrovich, and P. E. Burt, Phys. Rev. Lett. **65**, 547 (1990).
- [4] N. Tamimi, B. D. Anderson, A. R. Baldwin, T. Chittrakarn, M. Elaasar, R. Madey, D. M. Manley, M. Mostajabodda'vati, J. W. Watson, W.-M. Zhang, J. A. Carr, and C. C. Foster, Phys. Rev. C **45**, 1005 (1992).
- [5] S. Yen, R. J. Sobie, T. E. Drake, H. Zarek, C. F. Williamson, S. Kowalski, and C. P. Sargent, Phys. Rev. C **27**, 1939 (1983).
- [6] C. Olmer, A. D. Bacher, G. T. Emery, W. P. Jones, D. W. Miller, H. Nann, P. Schwandt, S. Yen, T. E. Drake, and R. J. Sobie, Phys. Rev. C **29**, 361 (1984).
- [7] M. Yasue, T. Tanabe, S. Kubono, J. Kokame, M. Sugitani, Y. Kadota, Y. Taniguchi, and M. Igarashi, Nucl. Phys. **A391**, 377 (1982).
- [8] H. Zarek, S. Yen, B. O. Pich, T. E. Drake, C. F. Williamson, S. Kowalski, and C. P. Sargent, Phys. Rev. C **29**, 1664 (1984).
- [9] R. A. Lindgren, B. L. Clausen, G. S. Blanpied, J. Hernandez, C. S. Mishra, W. K. Mize, C. S. Whisnant, B. G. Ritchie, C. L. Morris, S. J. Seestrom-Morris, C. Fred Moore, P. A. Seidl, B. H. Wildenthal, R. Gilman, and J. A. Carr, Phys. Rev. C **44**, 2413 (1991).
- [10] G. S. Adams, A. D. Bacher, G. T. Emery, W. P. Jones, R. T. Kouzes, D. W. Miller, A. Picklesimer, and G. E. Walker, Phys. Rev. Lett. **38**, 1387 (1977).
- [11] B. D. Anderson, B. Wetmore, A. R. Baldwin, D. Lamm, R. Madey, D. M. Manley, J. W. Watson, W. M. Zhang, C. C. Foster, and Y. Wang, IUCF Progress Report, 1993, p. 44.
- [12] W. B. Cottingham, K. G. Boyer, W. J. Braithwaite, S. J. Greene, C. J. Harvey, R. J. Joseph, D. B. Holtkamp, C. Fred Moore, J. J. Kraushaar, R. J. Peterson, R. A. Ristinen, J. R. Shepard, G. R. Smith, R. L. Boudrie, N. S. P. King, C. L. Morris, J. Piffaretti, and H. A. Thiessen, Phys. Rev. C **36**, 230 (1987).
- [13] R. S. Hicks, J. B. Flanz, R. A. Lindgren, G. A. Peterson, L. W. Fagg, and D. J. Millener, Phys. Rev. C **30**, 1 (1984).
- [14] D. B. Holtkamp, S. J. Seestrom-Morris, D. Dehnard, H. W. Baer, C. L. Morris, S. J. Greene, C. J. Harvey, D. Kurath, and J. A. Carr, Phys. Rev. C **31**, 957 (1985).
- [15] M. A. Plum, R. A. Lindgren, J. Dubach, R. S. Hicks, R. L. Huffman, B. Parker, G. A. Peterson, J. Alster, J. Lichtenstadt, M. A. Moinester, and H. Baer, Phys. Rev. C **40**, 1861 (1989).
- [16] D. F. Geesaman, D. Kurath, G. C. Morrison, C. Olmer, B. Zeidman, R. E. Anderson, R. L. Boudrie, H. A. Thiessen, G. S. Blanpied, G. R. Bureson, R. E. Segel, and L. W. Swenson, Phys. Rev. C **27**, 1134 (1983).
- [17] J. C. Bergstrom, R. Neuhausen, and G. Lahm, Phys. Rev. C **29**, 1168 (1984).
- [18] D. B. Holtkamp, W. J. Braithwaite, W. Cottingham, S. J. Greene, R. J. Joseph, C. F. Moore, C. L. Morris, J. Piffaretti, E. R. Siciliano, H. A. Thiessen, and D. Dehnard, Phys. Rev. Lett. **45**, 420 (1980).
- [19] C. E. Hyde-Wright, W. Bertozzi, T. N. Buti, J. M. Finn, F. W. Hersman, M. V. Hynes, M. A. Kovash, J. J. Kelly, S. Kowalski, J. Lichtenstadt, R. W. Lourie, B. E. Norum, B. Pugh, C. P. Sargent, B. L. Berman, F. Petrovich, and J. A. Carr, Phys. Rev. C **35**, 880 (1987).
- [20] B. L. Clausen, R. J. Peterson, C. Kormanyos, J. E. Wise, A. B. Kurepin, and Y. K. Gavrilov, Phys. Rev. C **48**, 1632 (1993).
- [21] M. A. Plum, Ph.D. thesis, University of Massachusetts, 1985.
- [22] C. Olmer, B. Zeidman, D. F. Geesaman, T.-S. H. Lee, R. E. Segel, L. W. Swenson, R. L. Boudrie, G. S. Blanpied, H. A. Thiessen, C. L. Morris, and R. E. Anderson, Phys. Rev. Lett. **43**, 612 (1979).
- [23] S. Yen, R. Sobie, H. Zarek, B. O. Pich, T. E. Drake, C. F. Williamson, S. Kowalski, and C. P. Sargent, Phys. Lett. **93B**, 250 (1980).
- [24] D. F. Geesaman, R. D. Lawson, B. Zeidman, G. C. Morrison, A. D. Bacher, C. Olmer, G. R. Bureson, W. B. Cottingham, S. J. Greene, R. L. Boudrie, C. L. Morris, R. A. Lindgren, W. H. Kelly, R. E. Segel, and L. W. Swenson, Phys. Rev. C **30**, 952 (1984).
- [25] R. A. Lindgren, J. B. Flanz, R. S. Hicks, B. Parker, G. A. Peterson, R. D. Lawson, W. Teeters, C. F. Williamson, S. Kowalski, and X. K. Maruyama, Phys. Rev. Lett. **46**, 706 (1981).
- [26] B. L. Clausen, J. T. Brack, M. R. Braunstein, J. J. Kraushaar, R. A. Loveman, R. J. Peterson, R. A. Ristinen, R. A. Lindgren, and M. A. Plum, Phys. Rev. C **41**, 2246 (1990).
- [27] R. A. Lindgren, M. A. Plum, W. J. Gerace, R. S. Hicks, B. Parker, C. F. Williamson, X. K. Maruyama, and F. Petrovich, Phys. Rev. Lett. **47**, 1266 (1981).
- [28] J. A. Carr, S. D. Bloom, F. Petrovich, and R. J. Philpott, Phys. Rev. C **45**, 1145 (1992).
- [29] S. J. Seestrom-Morris, Ph.D. thesis, University of Minnesota, 1981; Los Alamos National Laboratory Report No. LA-8916-T, 1981.
- [30] C. L. Morris, L. Atencio, R. L. Boudrie, and S. J. Greene, Los Alamos National Laboratory Progress Report No. LA-11670-PR, 1989, p. 158.
- [31] J. J. Kelly, computer code ALLFIT, 1987 (unpublished).
- [32] J. Piffaretti, R. Corfu, J.-P. Egger, P. Gretillat, C. Lunke, E. Schwarz, C. Perrin, and B. M. Freedom, Phys. Lett. **71B**, 324 (1977).
- [33] J. P. Albanese, J. Arvieux, J. Bolger, E. Boschitz, C. H. Q. Ingram, J. Jansen, and J. Zichy, Nucl. Phys. **A350**, 301 (1980).
- [34] B. Chabloz, R. Corfu, J.-P. Egger, J.-F. Germond, P. Gretillat, C. Lunke, J. Piffaretti, E. Schwarz, C. Perrin, J. E. Bolger, and J. Zichy, Phys. Lett. **81B**, 143 (1979).
- [35] R. A. Arndt and L. O. Roper, program SAID (Scattering Analysis Interactive Dialin), SM89.
- [36] J. A. Carr (private communication), concerning calculations in Ref. [28].
- [37] S. Suzuki, T. Saito, K. Takahisa, C. Takakuwa, T. Tohei, T. Nakagawa, J. Takamatsu, A. Terakawa, M. Fujiwara, and Y. Fujita, RCNP Annual Report 1989, Osaka University, 1990, p. 15.
- [38] P. M. Endt, Nucl. Phys. **A521**, 1 (1990).
- [39] M. Petraitis, J. P. Connelly, Hall Crannell, L. W. Fagg, J. T. O'Brien, D. I. Sober, J. R. Deininger, S. E. Williamson, R. Lindgren, and S. Raman, Phys. Rev. C **49**, 3000 (1994).
- [40] G. M. Crawley, C. Djalali, N. Marty, M. Morlet, A. Willis, N. Anantaraman, B. A. Brown, and A. Galonsky, Phys. Rev. C **39**, 311 (1989).
- [41] J. Kalifa, J. Vernotte, Y. Deschamps, F. Pougheon, G. Rot-

- bard, M. Vergnes, and B. H. Wildenthal, Phys. Rev. C **17**, 1961 (1978).
- [42] B. L. Clausen, R. J. Peterson, and R. A. Lindgren, Phys. Rev. C **38**, 589 (1988).
- [43] J. A. Carr, F. Petrovich, D. Halderson, and J. Kelly, 1981 version of the computer program ALLWRLD (unpublished).
- [44] J. A. Carr, 1981 version of the computer program MSUDWPI (unpublished); adapted from the computer program DWPI of R. A. Eisenstein and G. A. Miller, Comput. Phys. Commun. **11**, 95 (1976).
- [45] H. de Vries, C. W. de Jager, and C. de Vries, At. Data Nucl. Data Tables **36**, 495 (1987).
- [46] C. W. de Jager, H. de Vries, and C. de Vries, At. Data Nucl. Data Tables **14**, 479 (1974).
- [47] P. D. Kunz, distorted wave Born approximation code DWUCK4, University of Colorado (unpublished).
- [48] R. A. Lindgren, M. Leuschner, B. L. Clausen, R. J. Peterson, M. A. Plum, and F. Petrovich, Can. J. Phys. **65**, 666 (1987).
- [49] A. Amusa and R. D. Lawson, Phys. Rev. Lett. **51**, 103 (1983).
- [50] L. Zamick, Phys. Rev. C **29**, 667 (1984).
- [51] F. Petrovich, W. G. Love, A. Picklesimer, G. E. Walker, and E. R. Siciliano, Phys. Lett. **95B**, 166 (1980).
- [52] P. Blunden, B. Castel, and H. Toki, Z. Phys. A **312**, 247 (1983).
- [53] J. A. Carr, Bull. Am. Phys. Soc. **38**, 1859 (1993).
- [54] Dean Halderson, R. J. Philpott, J. A. Carr, and F. Petrovich, Phys. Rev. C **24**, 1095 (1981).
- [55] D. J. Rowe, S. S. M. Wong, H. Chow, and J. B. McGrory, Nucl. Phys. **A298**, 31 (1978).
- [56] J. A. Carr, Phys. Rev. C **49**, 2505 (1994).
- [57] B. S. Ishkhanov, I. M. Kapitonov, and A. V. Shumakov, Nucl. Phys. **A394**, 131 (1983).
- [58] James A. Carr, in *Spin and Isospin in Nuclear Interactions*, edited by S. W. Wissink *et al.* (Plenum, New York, 1991), p. 333.
- [59] R. A. Lindgren, C. F. Williamson, and S. Kowalski, Phys. Rev. Lett. **40**, 504 (1978).
- [60] L. Knox, R. A. Lindgren, B. L. Clausen, B. Berman, D. Zubanov, M. Farkhondeh, L. W. Fagg, and M. Manley, Bull. Am. Phys. Soc. **34**, 1812 (1989).
- [61] N. G. Goncharova, Fiz. Elem. Chastits At. Yadra **23**, 1715 (1992) [Sov. J. Part. Nucl. **23**, 748 (1992)].
- [62] S. Yen, T. E. Drake, S. Kowalski, C. P. Sargent, and C. Williamson, Phys. Lett. **289B**, 22 (1992).
- [63] J. Liu, A. D. Bacher, S. M. Bowyer, S. Chang, C. Olmer, E. J. Stephenson, S. P. Wells, S. W. Wissink, and J. Lisantti, IUCF Progress Report, 1993, p. 24.
- [64] L. W. Fagg, Rev. Mod. Phys. **47**, 683 (1975).
- [65] P. M. Endt and C. Van der Leun, Nucl. Phys. **A310**, 1 (1978).
- [66] G. Mairle and G. J. Wagner, Z. Phys. **258**, 321 (1973).
- [67] E. R. Siciliano and D. L. Weiss, Phys. Lett. **93B**, 371 (1980).
- [68] J. A. Carr, F. Petrovich, D. Halderson, D. B. Holtkamp, and W. B. Cottingham, Phys. Rev. C **27**, 1636 (1983).